J. Pharm. Pharmacol. 1997, 49: 1008–1018
Received April 23, 1997
Accepted June 5, 1997

Impulse–response Studies on Tracer Doses of [^{14}C]Lignocaine and its Multiple Metabolites in the Perfused Rat Liver

GEORGE D. MELLICK AND MICHAEL S. ROBERTS

University of Queensland, Department of Medicine, Princess Alexandra Hospital, Australia

Abstract

The outflow-concentration–time profiles for lignocaine (lidocaine) and its metabolites have been measured after bolus impulse administration of [^{14}C]lignocaine into the perfused rat liver.

Livers from female Sprague-Dawley rats were perfused in a once-through fashion with red-blood-cell-free Krebs-Henseleit buffer containing 0 or 2% bovine serum albumin. Perfusate flow rates of 20 and 30 mL min^{-1} were used and both normal and retrograde flow directions were employed. Significant amounts of metabolite were detected in the effluent perfusate soon after lignocaine injection. The early appearance of metabolite contributed to bimodal outflow profiles observed for total ^{14}C radioactivity. The lignocaine outflow profiles were well characterized by the two-compartment dispersion model, with efflux rate << influx rate. The profiles for lignocaine metabolites were also characterized in terms of a simplified two-compartment dispersion model. Lignocaine was found to be extensively metabolized under the experimental conditions with the hepatic availability ranging between 0·09 and 0·18. Generally lignocaine and metabolite availability showed no significant change with alterations in perfusate flow rate from 20 to 30 mL min^{-1} or protein content from 0 to 2%. A significant increase in lignocaine availability occurred when 1200 μM unlabelled lignocaine was added to the perfusate. Solute mean transit times generally decreased with increasing flow rate and with increasing perfusate protein content.

The results confirm that lignocaine pharmacokinetics in the liver closely follow the predictions of the well-stirred model. The increase in lignocaine availability when 1200 μM unlabelled lignocaine was added to the perfusate is consistent with saturation of the hydroxylation metabolic pathways of lignocaine metabolism.

Impulse–response techniques, particularly in the form of multiple indicator dilution (MID) experiments have been extensively used to study the disposition of a range of solutes in the liver. The solutes studied include markers of liver spaces (Goresky 1963, 1980, 1983; Goresky et al 1985) endogenous compounds such as D-glucose (Goresky & Nadeau 1974), D-galactose (Goresky et al 1973), D-lactate (Schwab et al 1979), noradrenaline (Goresky et al 1989), thyroid hormones (Luxon & Weisiger 1992), bilirubin (Wolkoff et al 1979; Gartner et al 1981), fatty acids (Ferraresi-Filho et al 1989, 1992), taurocholic acid (Roberts et al 1990), inorganic anions (Bracht et al 1981), preformed metabolites of drugs such as paracetamol sulphate (Goresky et al 1992) and conjugates of 4-methylumbelliferone (Miyauchi et al 1987).

Relatively little impulse–response data is available for highly extracted solutes, although the pharmacokinetic predictions of the models for hepatic elimination are known to be most divergent for these compounds (Pang & Rowland 1977b). In addition, although the availability of metabolites has been studied under a range of conditions (Pang et al 1986; St-Pierre et al 1992), limited information is available on their distribution in the liver. Studies on the influence of changing physiological conditions on hepatic drug metabolism and distribution have been most frequently obtained using steady-state infusion techniques (Goresky et al 1983; Tsao et al 1986; St-Pierre & Pang 1993). Impulse–response studies give greater insight into what happens inside the liver's 'black box' (Roberts & Rowland 1986). The exogenous compounds which have been studied using this method include monohydric alcohols (Schwab et al 1990), warfarin (Tsao et al 1986), enalaprilat (Schwab et al 1990), paracetamol (Pang et al 1995), lignocaine (Huet et al 1985, 1986), diazepam (Diaz-Garcia et al 1992), diclofenac (Evans et al 1993), salicylate (Hussein et al 1994), barbiturates (Chou et al 1993), phenol (Ballinger et al 1995) and aspirin (Mellick & Roberts 1996). The discrimination between hepatic-elimination models' prediction of availability is greatest for highly extracted solutes (Pang & Rowland 1977a). Lignocaine and monoethylglycine xylidide, its metabolite, have been the pivotal compounds used to show the superiority of the well-stirred model over the tube model in describing the effect of flow rate on hepatic extraction (Pang & Rowland 1977c; Ahmad et al 1983). Each of the studies examining the effect of flow on lignocaine extraction was performed under steady-state conditions. The aim of this study was to characterize the impulse–response profiles for lignocaine and its metabolites (Fig. 1) under a range of physiological conditions in the in-situ perfused rat liver. It was hoped to be able to use the data to develop further the applicability of hepatic-elimination models in the prediction of availability with varying physiological conditions.

Correspondence: M. S. Roberts, Department of Medicine, University of Queensland, Princess Alexandra Hospital, Woolloongabba 4102, Australia.

Materials and Methods

Chemicals

[^{14}C]Lignocaine hydrochloride (carbonyl ^{14}C, specific activity 0·1 mCi mL^{-1}) and [^{3}H]water (specific activity 1 mCi mL^{-1}) were purchased from NEN-DuPont (Boston, MA) and Amersham (Sydney, Australia), respectively. Emulsifier safe scintillation fluid was purchased from Packard (Groningen, Netherlands). Unlabelled lignocaine hydrochloride, mono-

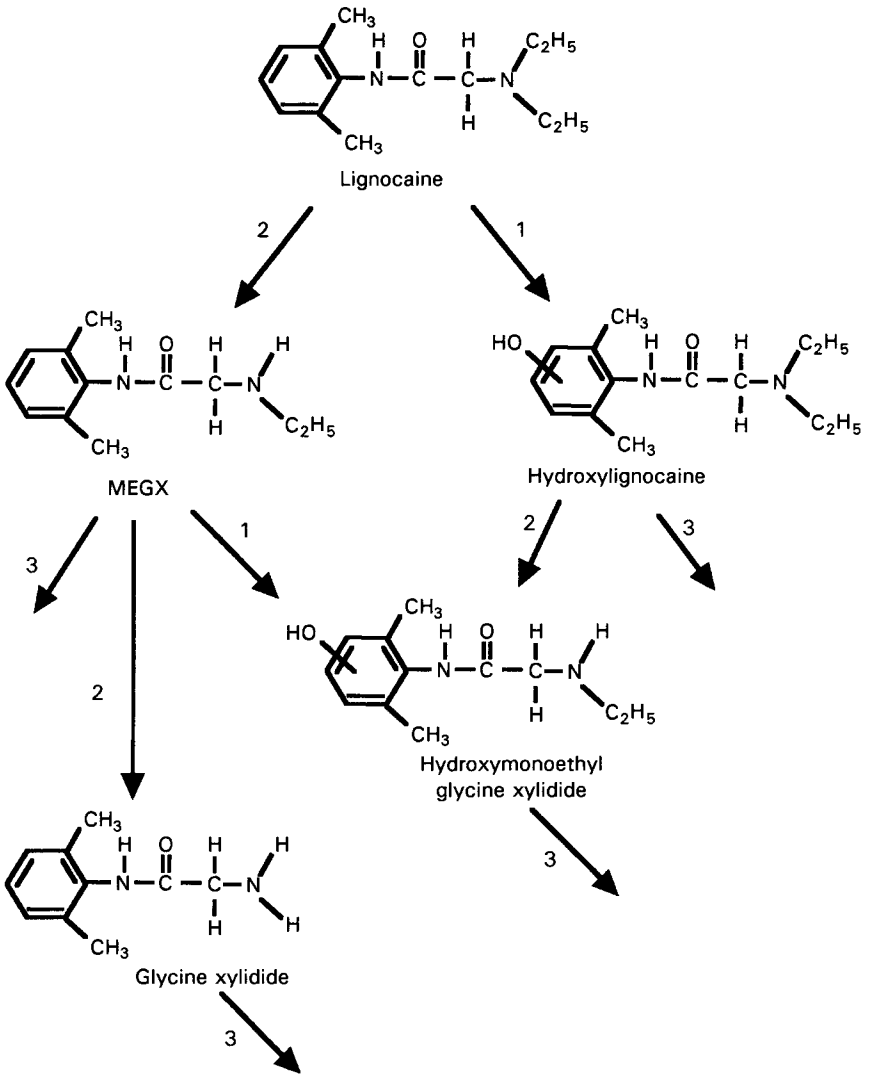

FIG. 1. Metabolic pathways for lignocaine metabolism. Lignocaine can undergo ring hydroxylation (1) to hydroxylignocaine, or deethylation (2) to MEGX. Hydroxymonoethylglycine xylidide is a common metabolite of both hydroxylignocaine and MEGX. Further deethylation of MEGX yields glycine xylidide (GX). Further metabolic pathways (3) include conjugation and amidolysis.

ethylglycine xylidide (MEGX) hydrochloride, hydroxylignocaine hydrochloride, hydroxymonoethylglycine xylidide hydrochloride and glycine xylidide hydrochloride were gifts from Astra Pharmaceuticals (Sodertalje, Sweden). Albumin (bovine-fraction V) was obtained from Sigma (St Louis, MO). Other reagents were of the highest grade available.

Liver perfusion

The in-situ perfused rat liver preparation used in this study has been described previously (Ballinger et al 1995; Mellick & Roberts 1996). Female Sprague-Dawley rats were used throughout. In these experiments, the perfusate consisted of red-blood-cell (RBC)-free Krebs-Henseleit buffer, pH 7·4, containing sodium chloride (118 mM), potassium chloride (4·74 mM), potassium dihydrogen phosphate (1·18 mM), magnesium sulphate heptahydrate (1·18 mM), calcium chloride dihydrate (2·54 mM), sodium bicarbonate (25 mM) and glucose (10 mM). The perfusate protein content was either 0 or 2% (w/w) bovine serum albumin (BSA). Flow rates of 20 and 30 mL min^{-1} $liver^{-1}$ were used in once-through perfusion with both normal and retrograde flow directions employed. In one group of experiments a background concentration of 1200 μM unlabelled lignocaine was included in the perfusate.

Impulse–response experiments

After commencement of liver perfusion, an initial stabilization period of 10 min was allowed. Bolus injections (50 μL), typically containing 1·8 μCi (10 μg) [^{14}C]lignocaine and 1 μCi [^{3}H]water in perfusate, were then introduced into the liver via the portal vein cannula. Evans Blue (1 mg mL^{-1}), a marker of the extracellular space, was included in injectates when albumin was present in the perfusate. Outflow samples from the liver were collected every second for 20 s and then every 4 s for a further 2 min. The outflow samples were then kept at 4°C until ready for analysis. Generally, two different perfusion conditions were employed per liver. In an additional set of experiments concerned with lignocaine and metabolite recovery, the outflow fractions were collected over 20 min after bolus injection of [^{14}C]lignocaine and analysed for total ^{14}C activity, i.e. lignocaine plus its metabolites. The cumulative

amount of radioactivity recovered in the bile after 20 min and the amount of ^{14}C activity in the liver after 20 min were also determined. The total amount of ^{14}C activity (perfusate outflow, bile and liver) was then compared with the dose of [^{14}C]lignocaine administered to estimate the total recovery.

Analysis of outflow samples

Outflow samples were analysed for total ^{14}C and ^{3}H radioactivity by adding 5 mL of emulsifier safe scintillation fluid to 20 μL of each sample and counted using a Minaxi β Tri-Carb 4000 series liquid scintillation counter (Packard Instruments, USA). For injections containing Evans Blue, 20 μL of each outflow sample was also removed for absorption spectrophotometric analysis of Evans Blue-labelled albumin at 620 nm using a Titertek multiskan MCC ELISA plate-counter. Generally, triplicate samples of at least two dilutions of the injectate (usually 1 in 50 and 1 in 100) were similarly analysed.

The remaining outflow samples were then used to assess the contribution of parent lignocaine and its various metabolites to the total ^{14}C radioactivity, using high-performance liquid chromatography (HPLC).

HPLC analysis

After analysis of the outflow samples as outlined above, consecutive samples collected over 1-s intervals were pooled in groups of five. These pooled samples and five other selected samples from the 4-s collections were prepared for HPLC analysis. Protein present in the samples was precipitated by addition of acetonitrile (acetonitrile/sample, 2 : 1). The acetonitrile solution used in the protein precipitation step contained unlabelled lignocaine and MEGX (both approximately 15 μg mL^{-1}) which acted as internal standards for HPLC. The samples were then centrifuged and the supernatant removed. The volume of supernatant was then reduced by evaporation in air to give a volume of approximately 50 μL which was injected directly on to the HPLC column. Separate recovery experiments showed that 89·7 ± 1·35% (mean ± s.e., n = 4) of the total ^{14}C radioactivity was recovered after protein precipitation and concentration. The [^{14}C]lignocaine was then separated from its metabolites by an HPLC assay adapted from that developed by Chen et al (1992).

The HPLC system consisted of a Waters 510 pump (flow rate 1·3 mL min^{-1}), model 710b automatic injector, model 480 UV detector (205 nm) and interface module (Waters, Millipore) and an NEC personal computer. A 5-μm Brownlea C_{18} reversed-phase HPLC column (Applied Biosystems, Foster City, CA) was employed with a mobile phase consisting of acetonitrile–0·05 M potassium dihydrogen phosphate, 15 : 85, containing 1% triethylamine, adjusted to pH 6 with orthophosphoric acid.

After injection (50 μL) of the prepared samples, 15-s fractions (0·325 mL) were collected from the HPLC column for 15–20 min by use of a Frac 100 fraction collector (Pharmacia, Sweden). Emulsifier safe scintillation fluid (8 mL) was added to each fraction which was then counted for ^{14}C radioactivity. It was then possible to determine the proportion of the total radioactivity in each sample corresponding to parent drug (lignocaine) and its various metabolites. All of the ^{14}C counts injected on to the HPLC column could be accounted for in the eluted fractions collected.

In the analysis of the bolus experiment data, the outflow-concentrations for lignocaine and metabolites were normalized to represent the fraction of total dose of lignocaine per mL of perfusate sample. All data are presented as mean ± standard error (n = 6) unless stated otherwise. The level of significance was based on $P < 0.05$.

Statistical moments analysis

The area under the solute-concentration–time curves (AUC), the area under the first-moment curve (AUMC) and the normalized variance of the outflow-concentration–time profiles were estimated using the parabolas-through–the-origin method (Purves 1992a, b, 1994) using the Moments Calculator 2·2 program developed by Robert Purves (University of Otago, New Zealand) for the Macintosh computer. The hepatic availability (F) for each solute was determined from the AUC values for the solutes using the equation:

$$F = Q\ AUC/D \quad (1)$$

where Q is the perfusate flow rate and D is the dose of solute administered. The mean transit time (MTT) of each solute was estimated from by the ratio of AUMC to AUC:

$$MTT = AUMC/AUC \quad (2)$$

The normalized variance of the outflow-concentration–time profiles (CV^2) was determined according to the equation:

$$CV^2 = \sigma^2/MTT^2 \quad (3)$$

where:

$$\sigma^2 = \int_0^\infty t^2 C(t)dt \Big/ \int_0^\infty C(t)dt - MTT^2 \quad (4)$$

Correction for catheter effects in moments analysis

The MTT and σ^2 determined from bolus studies is influenced by the passage of solute through the catheters used such that (Roberts et al 1990):

$$MTT_{total} = MTT_{liver} + MTT_{catheters} \quad (5)$$

and

$$\sigma^2_{total} = \sigma^2_{liver} + \sigma^2_{catheters} \quad (6)$$

Correction was made for catheter effects after determination of $MTT_{catheters}$ and $\sigma^2_{catheters}$ from a 'catheter' experiment performed identically to the liver experiments but in the absence of the organ. A bolus of [^{3}H]water was injected into the catheters and outflow collected each second for 30 s.

Two-compartment dispersion model analysis

Profiles of normalized outflow-concentration against time for lignocaine were analysed using a two-compartment dispersion model as previously described (Yano et al 1990; Evans et al 1993; Hussein et al 1994). Briefly, the profile of normalized outflow-concentration against time, C(t), from the liver can be described by the equation:

$$C(t)_{total} = I(t) * F(t)_{catheters} * F(t)_{liver} \quad (7)$$

where the symbol '*' denotes the convolution integral, I(t) is the input function for solute into the liver and $F(t)_{catheters}$ and $F(t)_{liver}$ are the transfer functions which describe the spread of transit times through the catheters and the liver, respectively.

In the Laplace domain, equation (7) is simplified with the convolution integral becoming multiplication and I(t) equalling unity for a bolus input:

$$C(s)_{total} = F(s)_{catheters} \times F(s)_{liver} \quad (8)$$

The transfer function $F(s)_{liver}$ for a non-eliminated extracellular reference solute such as albumin in the liver can be described using the one-compartment dispersion model (mixed boundary conditions) such that (Roberts & Rowland 1986):

$$F(s)_{liver} = \exp([1 - \sqrt{\{1 + 4D_N V_E s/Q\}}]/2D_N) \quad (9)$$

where D_N is the dispersion number for the liver, Q is the perfusate flow rate and V_E is the extracellular volume of the reference solute.

A similar equation can be used to describe the transfer function for the catheters:

$$F(s)_{catheters} = \exp([1 - \sqrt{\{1 + 4D_{CTH}V_{CTH}s/Q\}}]/2D_{CTH}) \quad (10)$$

Here D_{CTH} and V_{CTH} represent the dispersion number and the volume, respectively, of the catheters.

For a solute for which there is a permeability barrier in the liver the transfer function can be described using the two-compartment dispersion model (Yano et al 1990; Evans et al 1993):

$$F(s)_{liver} = \exp([1 - \sqrt{\{1 + 4D_N V_E s/Q(k_{12} + s - \{k_{21}k_{21}\}/\{s + k_{21} + k_{el}\})\}}]/2D_N) \quad (11)$$

where k_{12} and k_{21} represent the first-order influx and efflux rate-constants across the hepatocyte membrane and k_{el} represents the hepatocyte's first-order elimination rate-constant.

The influx, efflux and elimination rate-constants can be further defined:

$$k_{12} = PS\ f_{ub}/V_b \quad (12)$$

$$k_{21} = PS\ f_{uc}/V_c \quad (13)$$

$$k_{23} = CL_{int}\ f_{uc}/V_c \quad (14)$$

where PS is the permeability surface area product with the units of volume per time, f_{ub} and f_{uc} represent the unbound fraction of solute in blood and cells, respectively, and CL_{int} is the intrinsic clearance.

Albumin (extracellular reference) and the outflow profiles of the various solutes in the time domain were fitted to the appropriate transfer functions by numerical inversion of the Laplace equations using the Minim 3.0.8 non-linear parameter estimation program developed by Purves (1995). A Gauss Newton minimization algorithm was used with a weighting for all data points of $1/y_{observed}$. D_{CTH} and V_{CTH} were determined by fitting of the catheter outflow profile and these values were subsequently used for convolution of the catheter function for all other profiles. For the various solutes, the albumin reference profile was first fitted to the one-compartment dispersion equation to determine the D_N and the V_E for the particular injection. Then the solute profile was fitted using the two-compartment dispersion equation fixing the previously determined D_N and V_E values and estimating k_{12}, k_{21} and k_{el}. For injections which contained [^{3}H]water as the only reference solute, an extracellular curve was constructed from the water curve using the method of Goresky (1963), by appropriate adjustment of the concentration and time values for water by the factor which is the ratio of the average [^{3}H]water and Evans Blue-labelled albumin MTTs corrected for catheter transit time, determined at the same flow rate in the presence of albumin.

A simplified model for metabolite disposition based on equation (11) was used to fit and simulate the metabolite profiles, In this model, k_{12} for the metabolite is a hybrid constant representing both the uptake of the parent compound lignocaine into the cells and the conversion of the parent lignocaine to the metabolite. This model also assumes that the efflux of lignocaine from the cells and the influx of formed metabolite from the sinusoid back into liver cells is negligible.

Results

The experimental parameters associated with these liver-perfusion studies (n = 16) were: rat weight 210·6 ± 8·9 g and wet-liver weight 8·0 ± 0·2 g. The viability parameters were: oxygen consumption 0·80 ± 0·05 μmol min^{-1} g^{-1} liver; bile flow 0·81 ± 0·08 mg min^{-1} g^{-1} liver; perfusion pressure 7·8 ± 0·3 (n = 10) and 11·0 ± 0·8 cm water for flow rates of 20 and 30 mL min^{-1}, respectively. Catheter MTT were 0·97 and 0·91 s at flow rates of 20 and 30 mL min^{-1}, respectively.

Fig. 2 shows a typical radiochromatogram from a perfusate sample, showing the presence of lignocaine and its metabolites in the outflow perfusate after bolus injection of lignocaine. The HPLC procedure described was also used to determine that the purity of the stock [^{14}C]lignocaine was 96%.

The average outflow-concentration–time profiles for total ^{14}C radioactivity and the reference solutes at a flow rate of 20 mL min^{-1} and a perfusate protein content of 2% BSA are presented in Fig. 3A. The hepatic availability (F) for the reference solutes Evans Blue and [^{3}H]water approach unity (0·92 ± 0·07 and 0·98 ± 0·04, respectively) which is consistent with these solutes being non-extracted reference solutes. The MTT derived from statistical moments analysis for Evans Blue (15·48 ± 2·20 s) was significantly shorter than that for [^{3}H]water (30·77 ± 2·57 s) reflecting the different spaces occupied by these markers in the liver (extracellular and total water space, respectively). The CV^2 values for the reference solutes (Evans Blue 0·45 ± 0·18 and [^{3}H]water 0·65 ± 0·05) were also not significantly different from each another. At a flow rate of 30 mL min^{-1} the Evans Blue moments were:

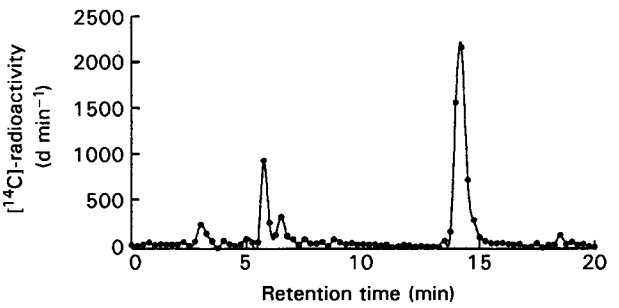

FIG. 2. Typical radiochromatogram of a protein-precipitated and concentrated outflow sample, obtained after bolus lignocaine injection into the perfused rat liver. Radiolabelled peaks corresponded to hydroxy MEGX (retention time 3 min), hydroxylignocaine (5·75 min), MEGX (6·5 min) and lignocaine (14·25 min).

$F = 0{\cdot}90 \pm 0{\cdot}06$, $MTT = 9{\cdot}03 \pm 0{\cdot}05$ s and $CV^2 = 0{\cdot}61 \pm 0{\cdot}13$ ($n = 3$).

Moments analysis of the total ^{14}C radioactivity curves yielded F, MTT and CV^2 values of $0{\cdot}42 \pm 0{\cdot}12$, $75{\cdot}80 \pm 2{\cdot}93$ and $0{\cdot}35 \pm 0{\cdot}07$, respectively. On average $7{\cdot}7 \pm 1{\cdot}2\%$ of the lignocaine dose was recovered as ^{14}C radioactivity in the bile.

Fig. 3B shows that along with lignocaine, the metabolites HL, MEGX and hydroxymethylglycine xylidide all contribute to the ^{14}C total radioactivity outflow profile. Approximately 25% of the total lignocaine dose was recovered as metabolites. Figs 3C–3F show how the amounts of lignocaine and each metabolite in the outflow perfusate vary with time, relative to total ^{14}C radioactivity. Very soon after injection, MEGX accounts for most of the ^{14}C radioactivity in the out-flowing perfusate (Fig. 3E), although lignocaine itself (Fig. 3F), hydroxylignocaine (Fig. 3D) and hydroxymonoethylglycine xylidide (Fig. 3C) also contribute to some extent. The contribution of lignocaine and hydroxylignocaine to the total radioactivity show similar time profiles with peaks between 40 and 60 s followed by a decline at longer times.

Fig. 4 shows the fitted curves for the outflow profiles of lignocaine and its metabolite MEGX from a typical injection of [^{14}C]lignocaine. Fitting of the extracellular reference curve (Evans Blue) yielded a CV^2 of $0{\cdot}42 \pm 0{\cdot}08$ and a MTT of $11{\cdot}50 \pm 1{\cdot}60$ s. The data are described quite well by the fitted curves with residuals being randomly distributed about zero. Table 1 summarizes the two-compartment dispersion model-fitting results. The choice of weighting data $1/y_{observed}$ (dotted line) did not significantly change the values of fitted parameters obtained when compared with unweighted fittings (solid line), although the fitted curves are slightly different (Fig. 4). Because the parameter estimations for hydro-

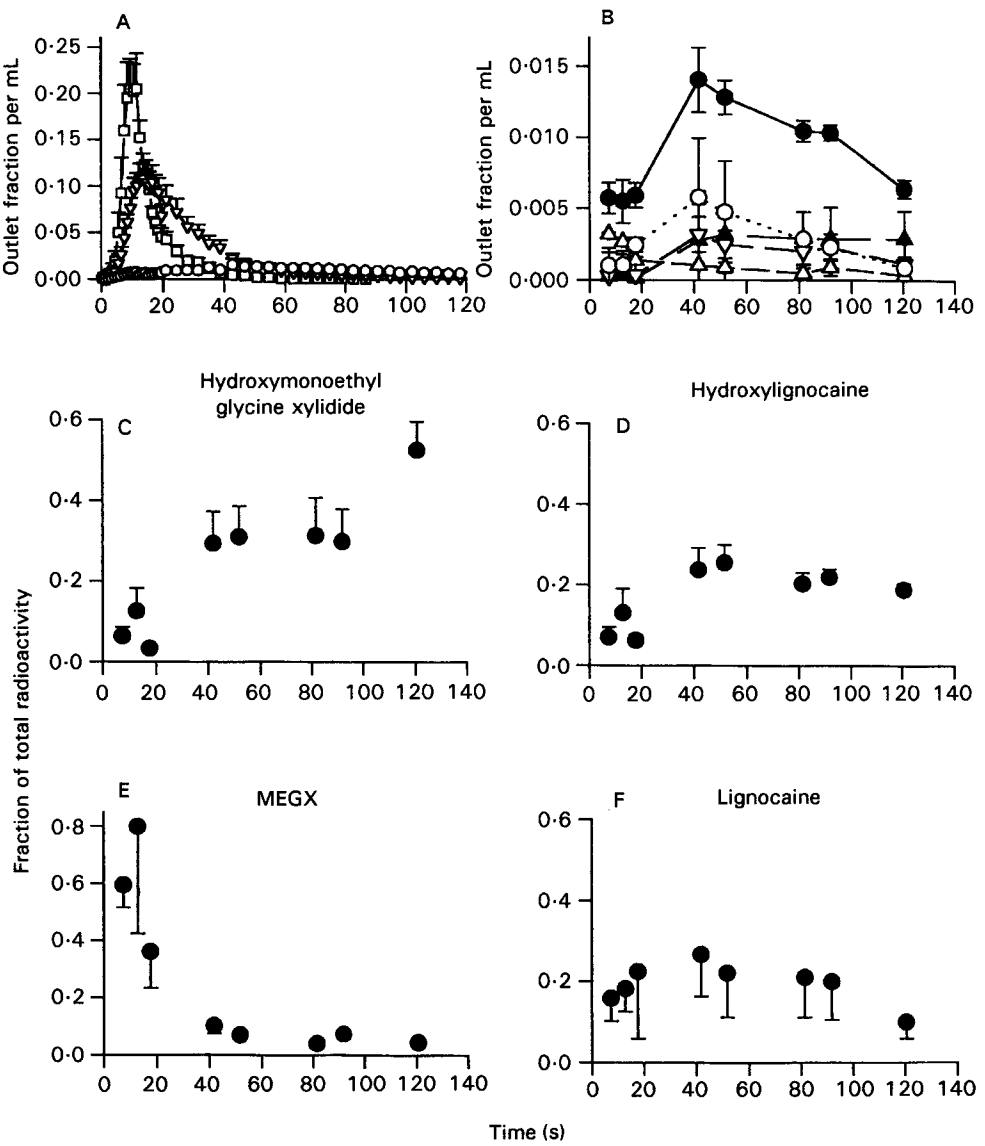

FIG. 3. Profiles of average outflow fraction against time at a flow rate of 20 mL min^{-1} and a protein content of 2% BSA after bolus impulse of [^{14}C]lignocaine into the perfused rat liver. A. total ^{14}C radioactivity (○), Evans Blue-labelled albumin (□) and [^{3}H]water (▽). B. total ^{14}C radioactivity (●) and its constituents lignocaine (○), MEGX (△), hydroxylignocaine (▽), and hydroxymonoethylglycine xylidide (▲), C. hydroxylignocaine radioactivity relative to the total, D. hydroxymonoethylglycine xylidide radioactivity relative to the total, E. MEGX radioactivity relative to the total, F. lignocaine radioactivity relative to the total.

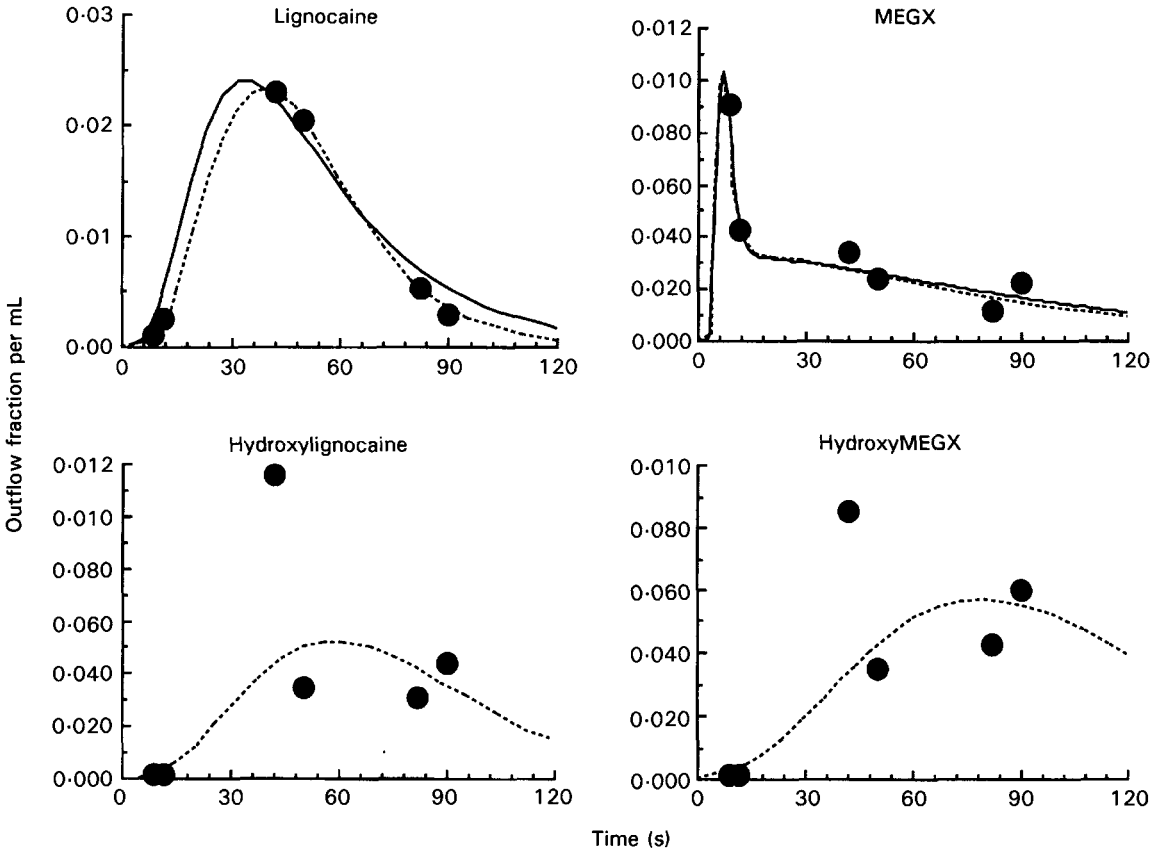

FIG. 4. Typical two-compartment dispersion model predicted outflow profiles for lignocaine and its metabolite MEGX unweighted (data and solid lines) and using weighting of $1/y_{obs}$ (dotted lines) after injection of [^{14}C]lignocaine. Given the sparse data for hydroxylignocaine and hydroxymonoethylglycine xylidide, parameter estimates were not recorded. The dotted lines shown in the figure are simulations based on the estimates determined by non-linear regression. Parameter values (s^{-1}) of 3·29, 0·34 and 0·02 were assumed for k_{12}, k_{21} and k_{el}, respectively, for hydroxylignocaine. The corresponding values for hydroxymonoethylglycine xylidide were assumed to be 2·21, 0·33 and 0·11. The metabolite simulations assume that metabolite formation is limited by lignocaine permeability and that uptake of formed metabolite from the sinusoid back into the cells is negligible.

xylignocaine and hydroxymonoethylglycine xylidide were unreliable owing to the small number of data points, these have not been reported in terms of parameter estimates. Shown in Fig. 4 are, however, simulations of hydroxylignocaine and hydroxymonoethylglycine xylidide plasma concentration–time profiles based on the crude regression estimates.

Fig. 5 shows the profiles of outflow fraction against time for lignocaine and metabolites under various perfusion conditions. The statistical moments results from the analysis of these profiles are presented in Table 2. For lignocaine and metabolites, no significant difference in F was observed between groups except when a background concentration of 1200 μM unlabelled lignocaine was present in the perfusate. In this case the availability of lignocaine (0·71 ± 0·09, n = 3) was significantly higher and the availability of hydroxylignocaine and hydroxymonoethylglycine xylidide (0·02 and 0·03) were significantly lower than those of the other groups. The availability of MEGX in this group and the other groups was not significantly different. MTT for all solutes was reduced as flow rate was increased from 20 to 30 mL min^{-1} and protein content was increased from 0 to 2%. The presence of 1200 μM unlabelled lignocaine in the perfusate tended to

Table 1. Two-compartment dispersion-model-fitting parameters for lignocaine and its MEGX metabolite obtained from fitting of outflow profiles represented in Fig. 4.

Solute	Parameter values			
	Influx rate constant (s^{-1})	Efflux rate constant (s^{-1})	Elimination rate constant (s^{-1})	Ratio of influx rate constant to efflux rate constant
Lignocaine	1·73 ± 0·49	0·19 ± 0·07	0·04 ± 0·01	9·4
Monoethylglycine xylidide	0·80 ± 0·16	0·20 ± 0·15	0·11 ± 0·07	4·0

The perfusion flow rate was 20 mL min^{-1} and the perfusate protein content was 2% BSA. Data are presented as mean ± s.e.

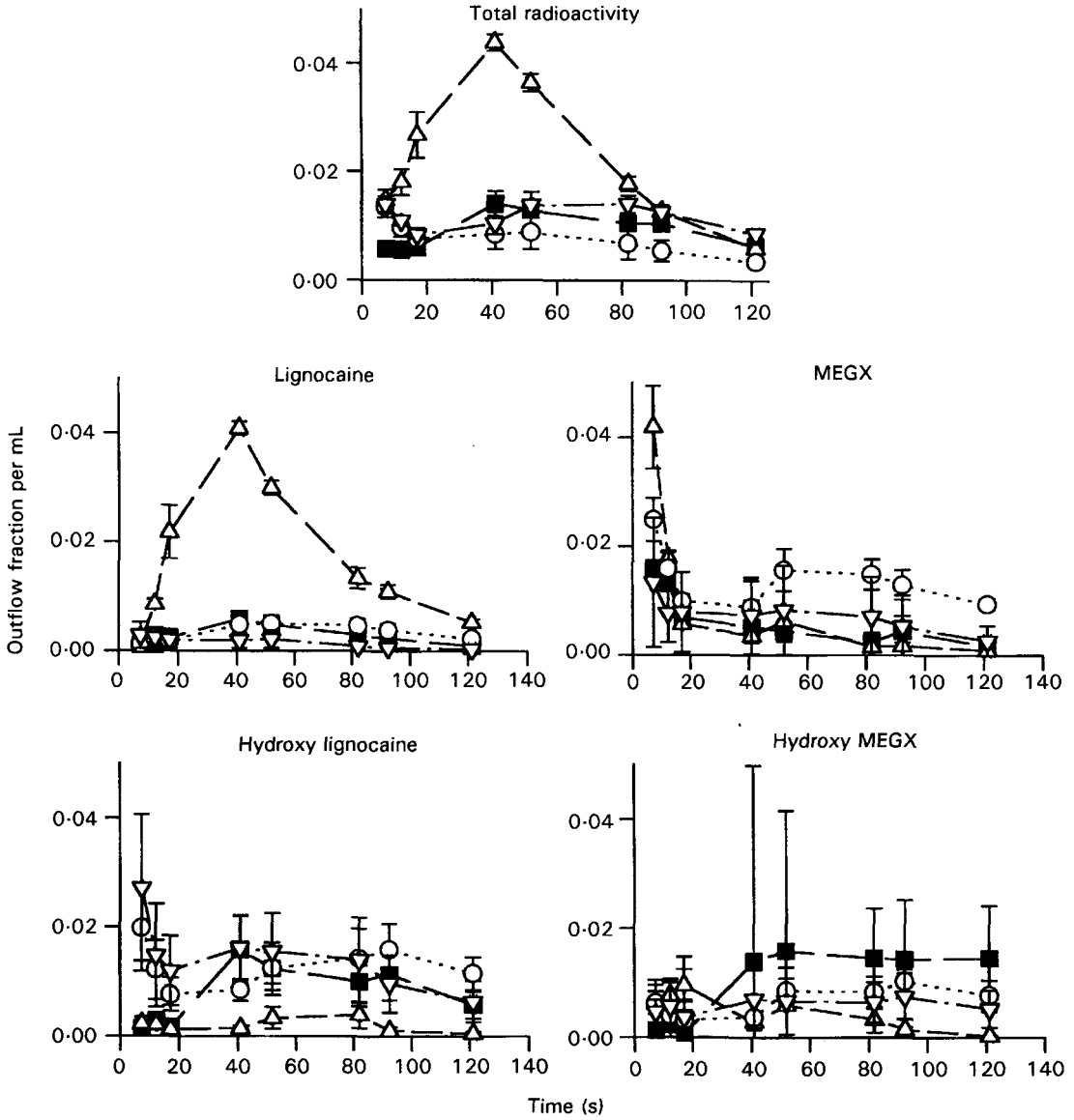

FIG. 5. Profiles of outflow fraction against time for total ^{14}C radioactivity, lignocaine, MEGX, hydroxylignocaine and hydroxymonoethylglycine xylidide under various conditions of perfusion: 20 mL min^{-1} 2% BSA (■); 20 mL min^{-1} 0% BSA in the presence of 1200 μM unlabelled lignocaine background in the perfusate (△); 30 mL min^{-1} 0% BSA (▽); 30 mL min^{-1} 2% BSA (○).

increase lignocaine MTT and reduce MTT for the metabolites. In general, the CV^2 values obtained (range 0·20 to 1·47) were similar in magnitude to those obtained for the reference solutes.

Analysis of the cumulative amount of total [^{14}C]lignocaine in the perfusate and bile after 20 min together with the amount of total ^{14}C recovered in the liver after the same time accounted for 101·1 ± 2·2% of the ^{14}C dose administered in the form of radiolabelled lignocaine. This total radioactivity was distributed in the perfusate outflow, bile and liver tissue as (mean ± s.d.) 88·7 ± 6·0, 9·8 ± 3·5 and 3·8 ± 2·1%, respectively, of the [^{14}C]lignocaine dose injected.

Discussion

Lignocaine is metabolized by two competing pathways; *N*-deethylation to yield monoethylglycine xylidide (MEGX) and ring hydroxylation yielding 3- or 4-hydroxylignocaine (Keenaghan & Boyes 1972), see Fig. 1. MEGX and hydroxylignocaine have a common metabolite in hydroxymonoethylglycine xylidide which can undergo further metabolism via conjugation or amidolysis. Similarly MEGX can undergo further metabolism via conjugation, amidolysis or further deethylation to glycine xylidide (GX) (Keenaghan & Boyes 1972). In the current study, the metabolites available to our group, hydroxylignocaine, MEGX and hydroxymonoethylglycine xylidide were all detected in the effluent perfusate after bolus administration of [^{14}C]lignocaine to the liver.

Bolus studies often utilize radiolabelled solutes to achieve tracer drug concentrations. This study shows the importance of considering the presence of radiolabelled metabolites in the effluent perfusate, even soon after injection. The impulse-response approach to the study of metabolite kinetics uses the

Table 2. Moments-analysis parameters for lignocaine and its metabolites after bolus administration of [^{14}C]lignocaine.

	Experimental group			
Flow rate = Protein =	20 mL min^{-1} 2% BSA (n = 6)	20 mL min^{-1} 0% BSA (n = 3)*	30 mL min^{-1} 0% BSA (n = 6)	30 mL min^{-1} 2% BSA (n = 3)
Lignocaine				
Hepatic availability	0·11 ± 0·06†	0·71 ± 0·09	0·10 ± 0·02	0·15 ± 0·03
Mean transit time (s)	62·78 ± 5·21	82·44 ± 12·29	61·57 ± 8·56	39·32 ± 1·27
Normalized variance of outflow-concentration–time profile	0·20 ± 0·04	0·24 ± 0·01	0·39 ± 0·06	0·40 ± 0·05
Hydroxylignocaine‡				
Hepatic availability	0·11	0·02	0·21	0·17
Mean transit time (s)	113·40	58·45	80·69	37·48
Normalized variance of outflow-concentration–time profile	0·51	0·27	0·72	0·70
Monoethylglycine xylidide‡				
Hepatic availability	0·05	0·05	0·09	0·03
Mean transit time (s)	68·84	33·20	63·43	42·64
Normalized variance of outflow-concentration–time profile	0·91	1·47	0·57	0·77
Hydroxymonoethylglycine xylidide‡				
Hepatic availability	0·09	0·03	0·11	0·12
Mean transit time (s)	74·83	42·50	109·79	99·80
Normalized variance of outflow-concentration–time profile	0·56	0·43	0·55	0·62

†Standard error. ‡Moments calculated from the average profiles (Fig. 5). *1200 μM unlabelled lignocaine background concentration in perfusate.

outflow profile of a solute from the liver after bolus administration to define the kinetic processes associated with solute movement into and out of cells, solute elimination and the transit time distribution of the solute molecules in the vascular space of the organ (Roberts & Rowland 1986; Yano et al 1989; Roberts et al 1990). The transit-time distribution for a non-extracted reference solute is indicative of the heterogeneity of flow rates and sinusoid lengths in the liver and the distribution of the solute in the liver. The transit-time distribution for total ^{14}C radioactivity represents the sum of unchanged [^{14}C]lignocaine and its metabolites eluting from the liver. The MEGX species is the component of ^{14}C radioactivity with the shortest transit time through the liver (Fig. 3). This rapid transit time reflects the smaller tissue distribution of MEGX relative to lignocaine and hydroxylignocaine as indicated by the smallest ratio k_{12}/k_{21} (Table 1). From equations (10) and (11), k_{12}/k_{21} is equivalent to $(f_{ub}V_c)/(f_{uc}V_b)$. A low ratio is therefore indicative of either a high fraction unbound in the cells or a restricted volume into which the MEGX can move. The elements of ^{14}C radioactivity which pass through the organ over the middle time-period (40–100 s after injection) are composed of lignocaine and all the metabolites, whereas the elements which have the longest passage through the organ consist predominantly of hydroxymonoethylglycine xylidide. Tam et al (1987) previously showed that after infusion of lignocaine into the rat liver MEGX levels peaked after approximately 5 min infusion with subsequent drop off to a steady-state concentration after approximately 60 min. At the same time lignocaine levels rose steadily reaching steady state between 50 and 60 min (Tam et al 1987). The hydroxylignocaine and hydroxymonoethylglycine xylidide concentration profiles after lignocaine infusion seemed to show trends similar to that of lignocaine (Tam et al 1987). Saville et al (1989) subsequently showed that the steady state was reached in 5–7 min when the liver was pretreated with lignocaine. Despite differences in the time scale, these observations after infusion of lignocaine show similarities to our results observed after bolus input.

The incomplete recovery of total ^{14}C dose in the effluent perfusate and bile in a 2·3-min period but with the majority (88·7%) being recovered in the perfusate after 20 min suggests slow wash out of lignocaine and its metabolites from the liver after injection of the precursor [^{14}C]lignocaine. The remaining lignocaine could be accounted for in the bile and liver tissue 20 min after dosing. Previous reports have alluded to the intracellular binding of lignocaine to microsomal proteins as a factor contributing to the well known time-dependent kinetics of this drug (Chen et al 1980; Tam et al 1987; Masubuchi et al 1992). In this study any time-dependent phenomena were minimized by use of tracer doses of lignocaine and by limiting liver exposure to only two lignocaine impulse–response studies per liver.

The two-compartment dispersion model can be used to describe the disposition of lignocaine and metabolites by use of an impulse-response study (Fig. 4). The limitation in the method by the small number of data points is because of the pooling required to analyse the low concentrations of lignocaine and metabolites. The MTT derived from fitting extracellular reference curves (11·50 s) is slightly shorter than, but consistent with, the estimated Evans Blue MTT determined using the model-independent statistical moments approach (15·48 s). Similarly, the D_N value obtained (0·21) from dispersion-model fitting is similar to that (0·23) obtained by the model-independent approach ($D_N = CV^2/2$).

The influx k_{12} (1·73 s^{-1}) and efflux k_{21} (0·19 s^{-1}) values for lignocaine are much lower than those reported by Saville et al (1992). Saville et al (1992), however, represented the vascular space of the liver by a well-stirred compartment as distinct from the dispersion model used in this and earlier studies

(Roberts et al 1988; Yano et al 1989; Chou et al 1993). The higher values of k_{12} and k_{21} reported by Saville et al (1992) might arise in part from this approximation because enzyme clearances predicted using the well-stirred model are also much higher than those predicted using either the dispersion or the tube models (Roberts & Rowland 1986). Result from this work and from that of Saville et al (1992) are consistent with efflux from the tissue compartment being a rate-controlling step. The ratio of k_{12}/k_{21} for this work and for that of Saville et al (1992) are 5·5 and 9·4, respectively. The elimination rate-constant in this tracer-dose study (Table 1) was expected to be higher than that obtained by Saville et al (1992), who infused relatively high lignocaine concentrations. A limitation of the current study was a lack of lignocaine concentration data in the time before the peak of the impulse–response curve for lignocaine. Higher k_{12} for lignocaine metabolites, relative to lignocaine, suggests that the k_{12} values obtained for lignocaine are underestimated.

Dispersion-model fitting of the lignocaine outflow profile for a background concentration of 1200 μM unlabelled lignocaine in the perfusate, yielded a k_{12} of 13·14 s^{-1} and a k_{21} of 5·70 s^{-1} ($k_{el} = 0$). These values are similar to those reported by Saville et al (1992) although the ratio of k_{12}/k_{21} is only 2·3.

The ratio of k_{12}/k_{21} for MEGX (Table 1) represents the binding and distribution of MEGX in the tissues ($k_{12}/k_{21} = (f_{ub}V_c)/(f_{uc}V_b)$). Saville et al (1992) obtained ratios of 3·9 and 6·2 for the disposition of exogenously administered MEGX and hydroxylignocaine, respectively.

Lignocaine removal by the liver is known to be extensive, with greater than 95% extraction (E) reported in previous studies of perfused rat liver (Shand et al 1975; Pang & Rowland 1977b; Pang et al 1986; Tam et al 1987). The current study also demonstrated extensive metabolism of lignocaine by the liver with the hepatic availability (F) of lignocaine found to be between 0·09 and 0·18 after doses of 10 μg and 37 ng, respectively. These F values correspond to extraction ratios of 91–82% which are of the order shown in previous reports. This study also showed that the availability of lignocaine was not significantly affected by the perfusate flow rate or protein content.

An increase in flow from 20 to 30 mL min^{-1} with 2% BSA yielded an increase in availability of 0·11 to 0·15 (Table 2). The well-stirred model predicts an increase from 0·11 to 0·16 whereas the tube model predicts an increase from 0·11 to 0·23. It has previously been shown that increases in flow rate can be associated with an increase in sinusoidal volume (Roberts et al 1990). In such circumstances dispersion-model predictions of availability lie closer to that of the well-stirred model than to that of the tube model (Roberts et al 1990). In the current work, however, no significant increase in sinusoidal volume was observed with increasing flow rate and the dispersion model predicts an increase from 0·11 to 0·20 which is intermediate between the well-stirred and tube models.

In relation to protein concentration, the F_{ub} for lignocaine in 2% BSA Krebs buffer is 0·66 (Wu et al 1995). Increases of F from 0·10 to 0·14 and from 0·10 to 0·22 are predicted for well-stirred and tube models, respectively, as the albumin concentration is increased from 0 to 2% at 30 mL min^{-1}. The dispersion model again gives intermediate predictions (an increase from 0·10 to 0·20). The corresponding observed change in F was from 0·10 to 0·15.

The current study showed that lignocaine availability was significantly increased by the presence of an unlabelled background lignocaine concentration of 1200 μM in the perfusate. This result demonstrates the non-linear elimination kinetics of lignocaine owing to saturation of one or more of the metabolic pathways. That MEGX availability seems to be independent of the unlabelled lignocaine background concentration suggests that the deethylation pathway has not been completely saturated. This suggestion is reasonable considering the report by Suzuki et al (1984) of a K_M of 595 μM for the deethylation of lignocaine from in-vitro microsomal studies; this is approximately half the unlabelled background lignocaine concentration in the current study. In contrast, the contributions of hydroxylignocaine and hydroxymonoethylglycine xylidide to total ^{14}C radioactivity in the effluent perfusate are extremely low in the presence of the background concentration of unlabelled lignocaine. This is consistent with the saturation of the hydroxylation pathway ($K_M = 1·78$ μM; Suzuki et al 1984).

These results are also similar to those described by Tam et al (1987) who monitored lignocaine and its metabolites during continuous infusions of lignocaine into the single-pass isolated perfused rat liver. These workers found that as the infusate lignocaine concentration was increased to 200 μM, hydroxylignocaine and hydroxymonoethylglycine xylidide levels reached saturation whereas MEGX levels continued to increase with lignocaine concentration, indicating linear metabolism (Tam et al 1987). The experiments of Tam et al (1987) also gave results similar to those obtained in the current bolus studies in terms of total material balance (i.e. the recovery of the administered lignocaine as either lignocaine or metabolite in the effluent). These workers found a total mass balance approaching 50% at steady state after an infusion of 9·6 μM. This value increased to approximately 100% when infusate concentration was increased to 187 μM (Tam et al 1987). Similarly, the present bolus studies showed total recovery of ^{14}C radioactivity to be between 42 and 64% for the tracer lignocaine doses (10 μg) and 98% when a 1200-μM background lignocaine concentration was present in the perfusate.

Summary

This paper presents profiles of outflow fraction against time for lignocaine and its metabolites MEGX, hydroxylignocaine and hydroxymonoethylglycine xylidide after bolus administration of [^{14}C]lignocaine to the in-situ perfused rat liver. Significant amounts of lignocaine metabolites were present in the effluent perfusate very soon after injection. A two-compartment dispersion model adequately described the lignocaine outflow profiles with influx rate coefficient $\gg$ than efflux coefficient and elimination coefficient. The metabolite profiles were also fitted to the two-compartment dispersion model assuming that formation of metabolite was dependent on lignocaine permeability to the cells, and that metabolite influx from the extracellular space into the cells was negligible. These metabolite fittings also yielded influx parameters greater than efflux and elimination parameters. Lignocaine was found to be extensively metabolized under the experimental conditions, with the hepatic availability found to be between 0·09 and 0·18. In general no significant differences in statistical moments results were obtained when perfusate flow rate was varied from 20 to

$30\,mL\,min^{-1}$ or when the protein content of the perfusate was changed from 0 to 2%. These results are consistent with previous reports that lignocaine pharmacokinetics in the liver closely follow the predictions of the well-stirred model. The presence of 1200 μM unlabelled lignocaine in the perfusate resulted in a significant increase in lignocaine availability and metabolite profiles which were consistent with the saturation of the hydroxylation metabolic pathways of lignocaine metabolism.

Acknowledgements

The National Health and Medical Research Council of Australia and the Queensland and Northern NSW Lions Kidney and Medical Research Foundation provided support for this study. We acknowledge advice from M. Weiss in relation to the referees' comments on the presentation of data for hydroxylignocaine and hydroxymonoethylglycine xylidide.

References

Ahmad, A. B., Bennett, P. N., Rowland, M. (1983) Models of hepatic drug clearance: discrimination between the 'well-stirred' and 'parallel-tube' models. J. Pharm. Pharmacol. 35: 219–224

Ballinger, L. N., Cross, S. E., Roberts, M. S. (1995) Availability and mean transit times of phenol and its metabolites in the isolated perfused rat liver: normal and retrograde studies using tracer concentrations of phenol. J. Pharm. Pharmacol. 47: 949–956

Bracht, A., Kelmer-Bracht, A., Schwab, A. J., Scholz, R. (1981) Transport of inorganic anions in perfused rat liver. Eur. J. Biochem. 114: 471–479

Chen, C. P., Vu, V. T., Cohen, S. D. (1980) Lidocaine uptake in isolated rat hepatocytes and effects of DL-propranolol. Tox. Appl. Pharmacol. 55: 162–168

Chen, Y., Potter, J. M., Ravenscroft, P. J. (1992) A quick, sensitive high-performance liquid chromatography assay for monoethylglycinexylidide and lidocaine in serum/plasma using solid-phase extraction. Ther. Drug Monit. 14: 317–321

Chou, C. H., Evans, A. M., Fornasini, G., Rowland, M. (1993) Relationship between lipophilicity and hepatic dispersion and distribution for a homologous series of barbiturates in the isolated perfused in situ rat liver. Drug. Metab. Disp. 21: 933–938

Diaz-Garcia, J. M., Evans, A. M., Rowland, M. (1992) Application of the axial dispersion model of hepatic drug elimination to the kinetics of diazepam in the isolated perfused rat liver. J. Pharmacokin. Biopharm. 20: 171–193

Evans, A. M., Hussein, Z., Rowland, M. (1993) Influence of albumin on the distribution and elimination kinetics of diclofenac in the isolated perfused rat liver: analysis by the impulse-response technique and the dispersion model. J. Pharm. Sci. 82: 421–428

Ferraresi-Filho, O., Ferraresi, M. L., Constantin, J., Ishii-Iwamoto, E. L., Schwab, A. J., Bracht, A. (1989) The influence of albumin on palmitate transport in the isolated perfused rat liver. Braz. J. Med. Biol. Res. 22: 139–143

Ferraresi-Filho, O., Ferraresi, M. L., Constantin, J., Ishii-Iwamoto, E. L., Schwab, A. J., Bracht, A. (1992) Transport and metabolism of palmitate in the rat liver. Net flux and unidirectional fluxes across the cell membrane. Biochim. Biophys. Acta 1103: 239–249

Gartner, U., Stockert, R. J., Morell, A. G., Wolkoff, A. W. (1981) Modulation of the transport of bilirubin and asialoorosomucoid during liver regeneration. Hepatology 1: 99–106

Goresky, C. A. (1963) A linear method for determining liver sinusoidal and extravascular volumes. Am. J. Physiol. 204: 626–640

Goresky, C. A. (1980) Uptake in the liver: the nature of the process. In: Javitt, N. B. (ed.) Liver and Biliary Tract Physiology I. University Park Press, Baltimore, pp 65–101

Goresky, C. A. (1983) Kinetic interpretation of hepatic multiple-indicator dilution studies. Am. J. Physiol. 245: G1–G12

Goresky, C. A., Nadeau, B. E. (1974) Uptake of materials by the intact liver. The exchange of glucose across the cell membranes. J. Clin. Invest. 53: 634–646

Goresky, C. A., Bach, G. G., Nadeau, B. E. (1973) On the uptake of materials by the intact liver. The transport and net removal of galactose. J. Clin. Invest. 52: 991–1009

Goresky, C. A., Gordon, E. R., Bach, G. G.(1983) Uptake of monohydride alcohols by liver: demonstration of a shared enzymic space. Am. J. Physiol. 244: G198–G214

Goresky, C. A., Bach, G. G., Wolkoff, A. W., Rose, C. P., Cousineau, D. (1985) Sequestered tracer outflow recovery in multiple indicator dilution experiments J. Hepatol. 5: 805–814

Goresky, C. A., Bach, G. G., Cousineau, D., Schwab, A. J., Rose, C., Lee, S., Goresky, S. (1989) Handling of tracer norepinephrine by the dog liver. Am. Physiol. Soc. 256: G107–G123

Goresky, C. A., Pang, K. S., Schwab, A. J., Barker III, F., Cherry, W. F., Bach, G. G. (1992) Uptake of protein-bound polar compound, acetaminophen sulfate, by perfused rat liver. Hepatology 16: 173–190

Huet, P. M., Villeneuve, J. P., Pomier-Layrartgues, G., Marleau, D. (1985) Hepatic circulation in cirrhosis. Clin. Gastroenterol. 14: 155–168

Huet, P. M., Pomier, G., Villeneuve, J. P., Varin, F., Viallet, A. (1986) Intrahepatic circulation in liver disease. Semin. Liver Dis. 6: 277–286

Hussein, Z., McLachlan, A. J., Rowland, M. (1994) Distribution kinetics of salicylic acid in the isolated perfused rat liver assessed using moments analysis and the two-compartment axial dispersion model. Pharm. Res. 11: 1337–1345

Keenaghan, J. B., Boyes, R. N. (1972) The tissue distribution, metabolism and excretion of lidocaine in rats, guinea pigs, dogs and man. J. Pharmacol. Exp. Ther. 180: 454–463

Luxon, B. A., Weisiger, R. A. (1992) A new method for quantitating intracellular transport: application to the thyroid hormone 3,5,3′-triiodothyronine. Am. J. Physiol. 263: G1–G9

Masubuchi, Y., Araki, J., Narimatsu, S., Suzuki, T. (1992) Metabolic activation of lidocaine and covalent binding to rat liver microsomal protein. Biochem. Pharmacol. 43: 2551–2557

Mellick, G. D., Roberts, M. S. (1996) The disposition of aspirin and salicylic acid in the isolated perfused rat liver: the effect of normal and retrograde flow on availability and mean transit time. J. Pharm. Pharmacol. 48: 738–743

Miyauchi, S., Sugiyama, Y., Sawada, Y., Morita, K., Iga, T., Hanano, M. (1987) Kinetics of hepatic transport of 4-methylumbelliferone in rats. Analysis by multiple indicator dilution method. J. Pharmacokin. Biopharm. 15: 25–38

Pang, K. S., Rowland, M. (1977a) Hepatic clearance of drugs I. Theoretical considerations of a 'well-stirred' model and a 'parallel-tube' model. Influence of hepatic bood flow, plasma and blood cell binding and the hepatocellular enzymatic activity on hepatic drug clearance. J. Pharmacokin. Biopharm. 5: 625–654

Pang, K. S., Rowland, M. (1977b) Hepatic clearance of drugs II. Experimental evidence of acceptance of the 'well-stirred' model over the 'parallel-tube' model using lidocaine in the perfused rat liver in situ preparation. J. Pharmacokin. Biopharm. 5: 655–680

Pang, K. S., Rowland, M. (1977c) Hepatic clearance of drugs III. Additional experimental evidence supporting the 'well-stirred' model using the metabolite (MEGX) generated from lidocaine under varying conditions in the perfused rat liver in situ preparation. J. Pharmacokin. Biopharm. 5: 681–699

Pang, K. S., Terrell, J. A., Nelson, S. D., Feuer, K. F., Clements, M. J., Endrenyi, L. (1986) An enzyme-distributed system for lidocaine metabolism in the perfused rat liver preparation. J. Pharmacokin. Biopharm. 14: 107–130

Pang, K. S., Barker III, F., Simard, A., Schwab, A. J., Goresky C. A. (1995) Sulfation of acetaminophen by the perfused rat liver: the effect of red blood cell carriage. Hepatology 22: 267–282

Purves, R. D. (1992a) Optimal numerical integration methods for estimation of area-under-the-curve (AUC) and area-under-the-moments-curve (AUMC). J. Pharmacokin. Biopharm. 20: 211–226

Purves, R. D. (1992b) Bias and variance of extrapolated tail areas for area-under-the-curve (AUC) and area-under-the-moments-curve (AUMC). J. Pharmacokin. Biopharm. 20: 501–510

Purves, R. D. (1994) Numerical estimation of the non-compartmental parameters variance (URT) and coefficient of variation (CVRT) of residence times. J. Pharm. Sci. 83: 202–205

Purves, R. D. (1995) Accuracy of numerical inversion of Laplace transformations for pharmacokinetic parametric estimations. J. Pharm. Sci. 84: 71–74

Roberts, M. S., Rowland, M. (1986) A dispersion model of hepatic elimination 1. Formulation of the model and bolus considerations. J. Pharmacokinet. Biopharm. 14: 227–261

Roberts, M. S., Donaldson, J. D., Rowland, M. (1988) Models of hepatic elimination: comparison of stochastic models to describe residence time distributions and to predict the influence of drug distribution, enzyme heterogeneity and systemic recycling on hepatic elimination. J. Pharmacokin. Biopharm. 16: 41–83

Roberts, M. S., Fraser, S., Wagner, A., McLeod L. (1990) Residence time distributions of solutes in the perfused rat liver using a dispersion model of hepatic elimination 1. Effect of changes in perfusate flow and albumin concentration on sucrose and taurocholate. J. Pharmacokin. Biopharm. 18: 209–234

St-Pierre, M. V., Pang, K. S. (1993) Kinetics of sequential metabolism I. Formation and metabolism of oxazepam from nordiazepam and temazepam in the perfused murine liver. J. Pharmacol. Exp. Ther. 265: 1429–1445

St-Pierre, M. V., Lee, P. I., Pang, K. S. (1992) A comparative investigation of hepatic clearance models: predictions of metabolite formation and elimination. J. Pharmacokin. Biopharm. 20: 105–145

Saville, B. A., Gray, M. R., Tam, Y. K. (1989) Evidence for lidocaine-induced enzyme inactivation. J. Pharm. Sci. 73: 1003–1008

Saville, B. A., Gray, M. R., Tam, Y. K. (1992) Experimental studies of transient mass transfer and reaction in the liver: interpretation with a heterogeneous compartment model. J. Pharm. Sci. 81: 265–271

Schwab, A. J., Bracht, A., Scholz, R. (1979) Transport of D-lactate in perfused rat liver. Eur. J. Biochem. 102: 537–547

Schwab, A. J., Barker III, F., Goresky, C. A., Pang, K. S. (1990) Transfer of enalaprilat across rat liver cell membranes is barrier-limited. Am. J. Physiol. 258: G461–G475

Shand, D. G., Kornhauser, O. M., Wilkinson, G. R. (1975) Effects of route of administration and blood flow on hepatic drug elimination. J. Pharmacol. Exp. Ther. 195: 424–432

Suzuki, T., Fujita, S., Kawai, R. (1984) Precursor-metabolite interaction in the metabolism of lidocaine. J. Pharm. Sci. 73: 136–138

Tam, Y. K., Yau, M., Berzins, R., Montgomery, P. R., Gray, M. (1987) Mechanisms of lidocaine kinetics in the isolated perfused rat liver. Drug Metab. Dispos. 15: 12–16

Tsao, S. C., Sugiyama, Y., Sawada, Y., Nagase, S. (1986) Effect of albumin on hepatic uptake of warfarin in normal and analbuminemic mutant rats: analysis by multiple indicator dilution method. J. Pharmacokin. Biopharm. 14: 51–64

Wolkoff, A. W., Goresky, C. A., Sellin, J., Gatmaitan, Z., Arias, I. M. (1979) Role of ligandin in transfer of bilirubin from plasma into liver. Am. J. Physiol. 236: E638–E648

Wu, Z. Y., Cross, S. E., Roberts, M. S. (1995) Influence of physicochemical parameters and perfusate flow rate on the distribution of solutes in the isolated perfused rat hind limb using the impulse-response technique. J. Pharm. Sci. 84: 1020–1027

Yano, Y., Yamaoka, K., Aoyama, Y., Tanaka, H. (1989) Two-compartment dispersion model for analysis of organ perfusion system of drugs by fast inversion Laplace transformation (FILT). J. Pharmacokin. Biopharm. 17, 179–202

Yano, Y., Yamaoka, K., Minamide, T., Nakagawa, T., Tanaka, H. (1990) Evaluation of protein binding effect on local disposition of oxacillin in rat liver by a two-compartment dispersion model. J. Pharm. Pharmacol. 42: 632–636.